Photoluminescence enhancement of Eu^{3+} by energy transfer from Bi^{2+} to Eu^{3+} in bismuth glass nanocomposites

Shiv Prakash Singh and Basudeb Karmakar*

Abstract

Bi^{2+}-enhanced photoluminescence of Eu^{3+} doped Bi^{0}-bismuth glass nanocomposites are demonstrated here. The generation of bismuth nanoparticles (NPs) and its typical surface plasmon resonance at 460 nm are controlled by the oxidative method instead of conventional reduction technique during melt-quench processing. TEM image evidences the presence of spherical Bi^{0} NPs of 10-15 nm sizes and SAED pattern reveals their crystalline rhombohedral phase formation. The enhanced photoluminescence of Eu^{3+} is found to occur at 613 and 703 nm due to $^{5}D_{0}{\rightarrow}^{7}F_{2}$ and $^{5}D_{0}{\rightarrow}^{7}F_{4}$ transitions respectively. We believe that it has happened due to energy transfer from Bi^{2+} to Eu^{3+}.

Glass Science and Technology Section, Glass Division, CSIR-Central Glass and Ceramic Research Institute, 196, Raja S.C. Mullick Road, Kolkata 700 032, West Bengal, India
***E-mail: basudebk@cgcri.res.in**

Introduction

Rare earth doped glasses have attracted much attention world wide for their extensive applications such as in glass lasers, optical fiber amplifiers, optoelectronic and memory devices, flat-panel displays, etc. The luminescent properties of Eu^{3+} have fascinated researchers as a dopant since they can emit red fluorescence with high luminescence efficiency under UV light excitation.[1] Many researchers have activated it to enhance the europium emission intensity by co-doping with either another rare earth or transition metal ions in different matrices. Moreover, enhancement of rare earth luminescence in presence of metal nanoparticles is again a very fascinating area for researchers. [2, 3] In this context, bismuth ions are one of efficient luminescent activator with applications in lasers and a sensitizer for some rare earth ions, and are nowadays being investigated.[4] However, the luminescence origin from bismuth ions is still unclear and hence is highly debated. Many reports are available for the enhancement of luminescence of Eu^{3+} in presence of Bi^{3+} as a sensitizer in various matrices.[5] But the enhancement of luminescence of Eu^{3+} in presence of other valance state of bismuth ion has not been reported previously.

In view of above, bismuth glasses are considered as one of the most important amongst the heavy metal oxide glasses as a host matrix for rare earths.[6] But the problem associated with these glasses is its dark-brown or black coloration due to formation of metallic bismuth (Bi^0) during melting.[7] These glasses are, therefore, restricted to a great extent for optical and photonic applications. Consequently, synthesis of transparent bismuth glasses by suppressing the formation of Bi^0 nanoparticles (NPs) in bismuth glasses is very important for both scientific as well as technological points of view.

Recently, we have reported the suppression of metallic bismuth formation in bismuth glasses by the oxidative process using KNO_3 and $KClO_4$.[8]

In this letter, we demonstrate the enhancement of emission intensity of Eu^{3+} ion by the Bi^{2+} ions during controlled formation of Bi^0 using $K_2S_2O_8$ as oxidizing agent in the B_2O_3-ZnO-Bi_2O_3-SiO_2-K_2O glass system.

Experimental

Glasses were prepared by the melt-quench technique with the composition (wt %) $19B_2O_3$-$23ZnO$-$45Bi_2O_3$-$9SiO_2$-$(4-x)K_2O$-$xK_2S_2O_8$ (where x is 0, 0.2, 1.0 and 3.0, and named as a, b, c, and d respectively). All the glasses were doped with 0.5 wt % of Eu_2O_3 and designated as e, f, g and h respectively. The composition of glass has also been provided in Table 1. Bi_2O_3, H_3BO_3, ZnO and K_2CO_3 from Loba Chemie; SiO_2 (Bremthaler/Quarzitwerk), $K_2S_2O_8$ (Merck) and Eu_2O_3 (Alfe Aesar) were used as raw materials. The batch for 25 g glass was melted in a silica crucible at 1100^oC for 30 min followed by casting and annealing at 420^oC for 2h in air.

The UV-Vis absorption spectra were recorded using Perkin-Elmer (Lambda 20) double beam UV-visible spectrophotometer. The X-ray diffraction patterns of the bulk samples were recorded in an X'pert Pro MPD diffractometer (PANalytical) operating at 40 kV and 30 mA using Ni-filtered CuKα radiation with the X'celerator with step size 0.05^0 (2θ) step time 0.5 s, from 5^0 to 90^0. The TEM and SAED images were taken using a FEI instrument (Tehnai-30, ST G^2) operating at an accelerating voltage of 300 kV. The fluorescence spectra were measured with a Perkin Elmer Luminescence

Spectrophotometer (Model LS55) exciting at 393 nm using a Xenon lamp as the excitation source.

Results and discussion

Figure 1 (A) shows the UV-Vis absorption spectra of a, b, c and d samples with increase in concentration of oxidant $K_2S_2O_8$ (0 to 3 wt %) in the glasses. The base glass is deep black in color, but the transparency increases with addition of $K_2S_2O_8$. The glass melted using 3 wt % of $K_2S_2O_8$ is highly transparent. The base glass reveals a very weak surface plasmon resonance (SPR) band (shown in inset) due to presence of huge amount of Bi^0 NPs. When 0.2 wt % $K_2S_2O_8$ has added to the base glass, the surface plasmon band has visualized very distinctly. The intensity of SPR band gradually decreases with addition of further amount of $K_2S_2O_8$ (up to 3.0 wt %). The observed broad absorption band at 460 nm is appeared due to the SPR of Bi^0 NPs.[7-9] The SPR comes up due to collective oscillation of conduction band electrons of metallic nanoparticles embedded in dielectric host in response to optical excitation. Peng et $al.$[7] have found a broad absorption peak around 465 nm for Bi_2O_3 contained glasses and assigned the peak as surface plasmon resonance (SPR) of metallic bismuth. Singh et $al.$[8] and Khonthon et $al.$[9] have also described such absorption band of Bi^0 NPs at 460 nm in the different glass matrices, which correlates well with the present result. The UV-Vis absorption spectra of the glasses containing a constant amount of Eu_2O_3 (0.5 wt %) are also shown in the Fig. 1 (B). They exhibit characteristic absorption bands of Eu^{3+} at 393 and 464 nm which are attributed to transitions from $^7F_0$ to $^5L_6$ and $^5D_2$ states respectively as well as broad SPR band at 460 nm.[1] The intensity of SPR band gradually decreases with addition of oxidant

$K_2S_2O_8$, but the characteristic absorption bands of Eu^{3+} remain unchanged in all the glasses (e-h).

The significant effects of strong oxidizing agent $K_2S_2O_8$ are, therefore, the controlled generation of Bi^0 NPs and its SPR which results in the elimination of blackening color of bismuth glasses. By comparing the standard reduction potentials,[10] it is clear that the standard reduction potential of $S_2O_8^{2-}/SO_4^{2-}$ (2.01 V) is much higher than that of Bi^+/Bi^0 (0.50 V), Bi^{3+}/Bi^0 (0.31 V), Bi^{3+}/Bi^+ (0.20 V) and Bi^{3+}/Bi^{2+} (<0.20 V) species. Consequently, it easily favors the suppression of the formation of Bi^0 NPs and the glasses gradually become more transparent with increasing $K_2S_2O_8$ content.

Figure 2 shows the XRD pattern of the glass obtained by using 0.2 wt. % of $K_2S_2O_8$ (Glass b) as a representative. Although the glasses have not shown very distinct XRD patterns, the unresolved peaks depict around 27.63 and 28.78 degree 2θ indicate the existence of d_{116} and d_{122} Miller planes of rhombohedral metallic bismuth (JCPDS file no. 01-0699). However, TEM image (Fig. 3) of the same glass (Glass b) confirms the clear existence of bismuth nanoparticles. The TEM image shows 10-15 nm size of bismuth nanoparticles. The selected area electron diffraction (SAED) patterns inserted in the inset of Fig. 3, show d_{104} and d_{012} planes of bismuth nanoparticles correspond to rhombohedral crystal system (JCPDS file no. 85-1330). These results of TEM and SAED pattern again support that the glass contained Bi^0 NPs and correlated well with the SPR of Bi^0 NPs.

In Fig. 4 (A), emission spectra were obtained at 587, 613, 652 and 703 nm due to $^5D_0{\rightarrow}^7F_1$, $^5D_0{\rightarrow}^7F_2$, $^5D_0{\rightarrow}^7F_3$, and $^5D_0{\rightarrow}^7F_4$ transitions respectively of Eu^{3+} when excited by 393 nm at a fixed concentration of Eu^{3+} for all samples (e, f, g and h). These emission spectra compared with the base glass, it is observed that a peak has appeared at 703 nm in

the base glass. This peak is also present in the glasses containing Eu^{3+} ion. To examine the origin of this peak, the emission spectra of all the glasses without containing Eu^{3+} has been analyzed. In Fig. 4 (B), the emission spectra at 703 nm of the glasses a, b, c and d has been recorded by excitation at 393 nm. This emission intensity at 703 nm increases with decrease in the intensity of SPR band of bismuth nanoparticles. The excitation spectra at 393 nm for the glasses a, and d have been shown in Fig. 5 to examine the origin of the emission center at 703 nm. The composition and emission centers have also been listed in Table 1. Here, the emission intensity significantly increases with the concentration of $K_2S_2O_8$. Therefore, it is reasonable to believe that some emission center of bismuth gradually formed due to oxidation process during suppression of Bi^0 formation. Various researchers have reported about the different emission centers for the different valence state of bismuth such as Bi^{3+}, Bi^{2+} and Bi^+.[11-18] However, it is difficult to predict the exact valence state of Bi ion formed during melting process as their reduction potentials are very close to each other as indicated earlier.

The typical luminescence spectra of Bi^{3+} centered in the blue to green region when excited in the UV region has been reported by some researchers.[11, 12] The emission due to Bi^+ has been reported in NIR region.[12-14] Zhou *et al.*[12] have found emission due to Bi^+ ion in the NIR region centered at 1100 and 1400 nm when exited at 532 and 800 nm respectively. Peng *et al.*[13] have demonstrated NIR emission centered at 1250 nm in the BBSPS glasses, upon optical excitation at 785 nm and this emission center ascribed to Bi^+ species. The energy levels of Bi^0 was explained by Peng *et al.*[15] and they assigned red and NIR emission bands due to Bi^0 at 630 nm and 843 nm to electron transition $^2D_{5/2}$ $\rightarrow ^4S_{3/2}$ and $^2D_{3/2} \rightarrow ^4S_{3/2}$ respectively. But, in this study, the luminescence due to Eu^{3+}

increases instead of decrease with the decrease in Bi^0 concentration. Therefore, here the possibility of the emission band at 703 nm could not be assigned to Bi^{3+}, Bi^+ or Bi^0 species.

Hamstra et al.[16] have suggested the red luminescence due to Bi^{2+} ion, varying in the range of 17100-16000 cm^{-1} (585-625 nm) in the alkaline earth metal sulfates. Ren et al.[17] have exposed the visible luminescence spectra excited in the range 400-650 nm. The observed luminescence, when excited within this range, consists of two bands centered between 650 and 760 nm respectively. They assigned this red luminescence as characteristic spectra of Bi^{2+}. Such red luminescence bands arise from the electron transition between the first excited level $^2P_{3/2}$ (1) and ground level $^2P_{1/2}$ of Bi^{2+}. Because the absorption band observed by them is about 500 nm and the red luminescence from the glass are almost the same with the absorption and luminescence from Bi^{2+} activated crystals. They have ascribed this peak to the electron transition $^2P_{1/2} \rightarrow {}^2P_{3/2}$ and $^2P_{3/2} \rightarrow {}^2P_{1/2}$, respectively. Zhou et al.[12] have also reported the red emission due to Bi^{2+} ion. Taking into account all the above arguments, it is reasonable to assign the observed emission band at 703 nm to the emission of Bi^{2+} ions.

Emission intensity of Eu^{3+} ions in Fig. 4 (A) increased monotonically with the concentration of $K_2S_2O_8$ as shown in the inset, evidencing the energy transfer (ET) mechanism from Bi^{2+} to Eu^{3+} ions. Such energy transfer mechanism can also be well understood from the excitation spectra of the glass a, and d as shown in Fig. 5. The glasses a, and d revealed the excitation center at 393 nm for the emission at 703 nm which also matched well with the excitation wavelength of Eu^{3+}. Hence, upon excitation at 393 nm, both Bi^{2+} and Eu^{3+} ions are simultaneously excited from their ground levels to

the respective higher energy levels $^2P_{3/2}$ *(2)* and $^5L_6$. The energy level diagram of Bi^{2+} and Eu^{3+} ions and possible energy transfer process are schematically presented in Fig. 6. An excited Bi^{2+} ion relaxes from $^2P_{3/2}$ *(2)* to $^2P_{3/2}$ *(1)* state nonradiatively and transfers the energy to a neighboring $^5D_0$ level of Eu^{3+} ions, which is energetically close to each other. Thus, it (Bi^{2+}) enhances the emission intensities of $^5D_0 \rightarrow {}^7F_2$ and $^5D_0 \rightarrow {}^7F_4$ transitions of Eu^{3+} ions at 613 and 703 nm respectively. Similar study has been carried out by Guo *et al.*[19]. They have systematically investigated the energy transfer mechanism between luminescent centers of molecule-like, non-plasmonic Ag particles (ML-Ag-particles) and Eu^{3+}. They have demonstrated that upon 347 nm excitation, ML-Ag-particles are excited from the ground state to the excited state. Because the excited state of ML-Ag particles and the $^5L_6$ level of Eu^{3+} ions are energetically close to each other, energy transfer from ML-Ag-particles to Eu^{3+} ions can easily proceed.

Conclusions

Eu^{3+} doped Bi^0-bismuth glasses nanocomposites containing Bi^{2+} were prepared. Luminescence investigations revealed the enhancement of emission intensity of Eu^{3+} ion. This enhancement in the emission intensity supposed to be due to energy transfer from Bi^{2+} to Eu^{3+} ion. This is the first demonstration of energy transfer from Bi^{2+} to Eu^{3+} ions in bismuth glass. We believe that these findings would certainly facilitate more study on luminescence property of bismuth active centers and its application in photonics.

Acknowledgements

References

1 C. A. Kodaira, H. F. Brito, O. L. Malta, O. A. Serra, *J. Lumin.*, 2003, **101,** 11.

2 M. Wu, J. R. Lakowicz, C. D. Geddes, *J. Fluorescence*, 2005, **15**, 53.

3 Q. Wang, F. Song, C. Ming, H. Zhao, J. Liu, C. Zhang, S. Lin, E. Y. B. Pun, *J. Opt. Soc. Am. B*, 2011, **28** 220.

4 J. Ruan, E. Wu, H. Zeng, S. Zhou, G. Lakshminarayana, J. Qiu, *Appl. Phys. Lett.*, 2008, **92**, 101121.

5 L. Chen, Y. Jiang, Y. Yang, J. Huang, J. Shi, S. Chen, *J. Phys. D: Appl. Phys.*, 2009, **42**, 215104.

6 G. F. Yang, D. M. Shi, Q. Y. Zhang, Z. H. Jiang, *J. Fluorescence*, 2008, **18**,131.

7 M. Peng, C. Zollfrank, L. Wondraczek, *J. Phys.: Condens. Matter.*, 2009, **21**, 285106 1.

8 S. P. Singh, B. Karmakar, *Mater. Chem. Phys.*, 2010, **119**, 355.

9 S. Khonthon, S. Morimoto, Y. Arai, Y. Ohishi, *Opt. Meter.*, 2009, **31**, 1262.

10 P. Vanýsek, Electrochemical Series, in *CRC Hand Book of Chemistry and Physics*, CRC Press, London, p. 22, 1994.

11 X. T. Wei, Y. H. Chen, X. R. Cheng, M. Yin, W. Xu, *Appl. Phys. B*, 2010, **99**, 763.

12 S. Zhou, N. Jiang, B. Zhu, H. Yang, S. Ye, G. Laksminarayana, J. Hao, J. Qiu, *Adv. Funct. Mater.* 2008, **18**, 1407.

13 M. Peng, Q. Zhao, J. Qiu, L. Wondraczek, *J. Am. Ceram. Soc.* 2009, **92**, 542.

14 Y. Arai, T. Suzuki, Y. Ohishi, S. Morimoto, S. Khonthon, *Appl. Phys. Lett.*, 2007, **90**, 261110.

15 M. Peng, C. Zollfrank, L. Wondraczek, *J. Phys.: Condens. Matter.*, 2009, **21**, 285106
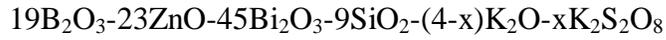
   1.

16 M. A. Hamstra, H. F. Folkerts, G. Blasse, *J. Mater. Chem.*, 1994, **4**, 1349.

17 J. Ren, G. Dong, S. Xu, R. Bao, J. Qiu, *J. Phys. Chem. A*, 2008, **112**, 3036.

18 H. Sun, Y. Sakka, M. Fujii, N. Shirahata, H. Gao, *Opt. Lett.*, 2011, **36**, 100.

19 H. Guo, X. F. Wang, J. D. Chen, F. Li, *Opt. Express*, 2010, **18**, 18900.

Table 1 Chemical composition of the glass and emission centers in the system (wt. %):

19B$_2$O$_3$-23ZnO-45Bi$_2$O$_3$-9SiO$_2$-(4-x)K$_2$O-xK$_2$S$_2$O$_8$

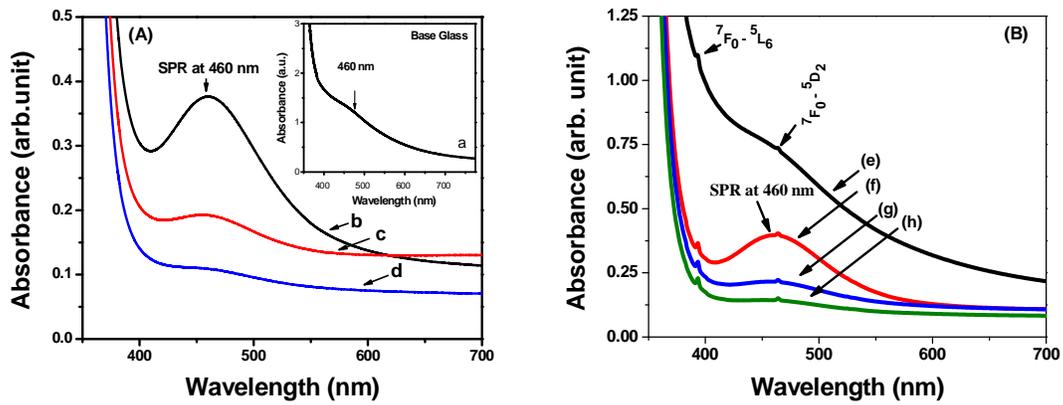| Glass identity	Oxidant, K$_2$S$_2$O$_8$ content, x, wt. %	Concentration of Eu$_2$O$_3$ in excess, wt. %	Emission center, nm
a	0.0	-	703
b	0.2	-	703
c	1.0	-	703
d	3.0	-	703
e	0.0	0.5	587, 613, 652, 703
f	0.2	0.5	587, 613, 652, 703
g	1.0	0.5	587, 613, 652, 703
h	3.0	0.5	587, 613, 652, 703

Figure captions

Fig. 1 (Color online) Absorption spectra of glasses (A) without and (B) with Eu_2O_3 contained glasses. For composition, see Table1.

Fig. 2 X-ray diffraction pattern of the glass obtained by using 0.2 wt. % of $K_2S_2O_8$.

Fig. 3 TEM image of the glass containing 0.2 wt % of $K_2S_2O_8$. Its SAED pattern (inset) shows <104> and <012> <hkl> planes of rhombohedral bismuth (JCPDS file 85-1330).

Fig. 4 (Color online) Photoluminescence (PL) spectra for excitation at 393 nm of (A) with and (B) without Eu_2O_3 contained glasses. In insets of (A) and (B), the PL intensities have shown as a function of concentration of $K_2S_2O_8$. For composition, see Table1.

Fig. 5 Photoluminescence excitation (PLE) spectra for emission at 703 nm. For composition, see Table1.

Fig. 6 Schematic representation of energy transfer from Bi^{2+} to Eu^{3+} in bismuth glass.

Fig. 1 (Color online) Absorption spectra of glasses (A) without and (B) with Eu_2O_3 contained glasses. For composition, see Table1.
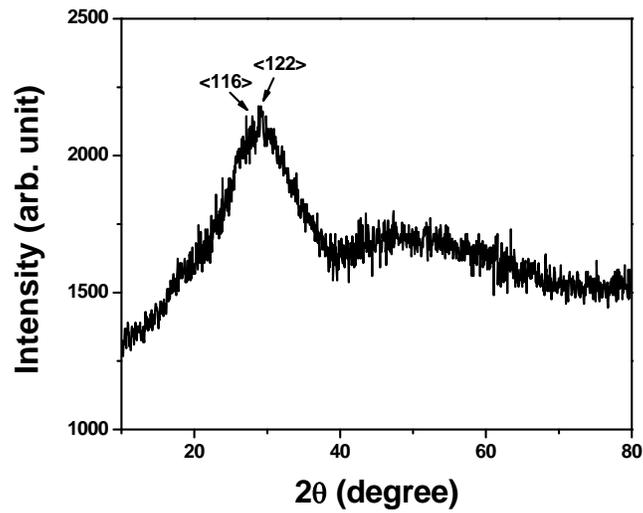

Fig. 2 X-ray diffraction pattern of the glass obtained by using 0.2 wt. % of $K_2S_2O_8$.

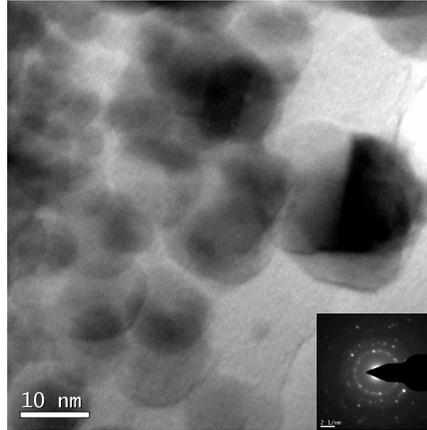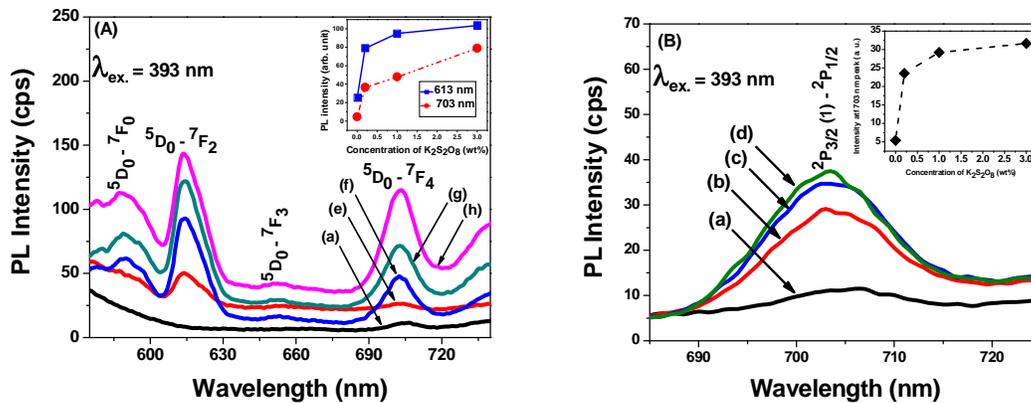**Fig. 3** TEM image of the glass containing 0.2 wt % of $K_2S_2O_8$. Its SAED pattern (inset) shows <104> and <012> <hkl> planes of rhombohedral bismuth (JCPDS file 85-1330).

Fig. 4 (Color online) Photoluminescence (PL) spectra for excitation at 393 nm of (A) with and (B) without Eu_2O_3 contained glasses. In insets of (A) and (B), the PL intensities have shown as a function of concentration of $K_2S_2O_8$. For composition, see Table1.
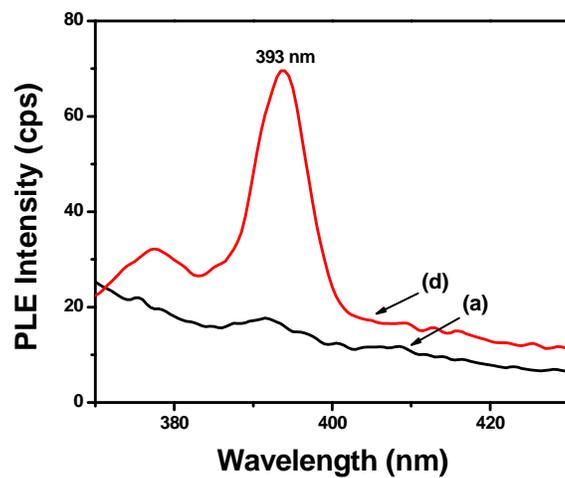
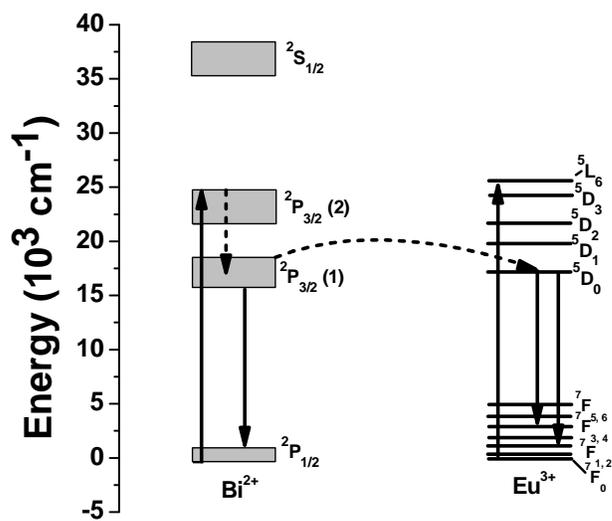**Fig. 5** Photoluminescence excitation (PLE) spectra for emission at 703 nm. For composition, see Table1.

Fig. 6 Schematic representation of energy transfer from Bi^{2+} to Eu^{3+} in bismuth glass.